Tunable Stochasticity in an Artificial Spin Network

Dédalo Sanz-Hernández, Maryam Massouras, Nicolas Reyren, N. Rougemaille, Vojtěch Schánilec, Karim Bouzehouane, Michel Hehn, Benjamin Canals, Damien Querlioz, Julie Grollier, et al.

A nano-magnetic Galton board

Dédalo Sanz-Hernández[1,†,*], Maryam Massouras[2,†], Nicolas Reyren[1], Nicolas Rougemaille[3], Vojtěch Schánilec[3,4], Karim Bouzehouane[1], Michel Hehn[2], Benjamin Canals[3], Damien Querlioz[5], Julie Grollier[1], François Montaigne[2], Daniel Lacour[2]

[1] Unité Mixte de Physique, CNRS, Thales, Université Paris-Saclay, 91767, Palaiseau, France
[2] Université de Lorraine, CNRS, Institut Jean Lamour, F-54000 Nancy, France
[3] Université Grenoble Alpes, CNRS, Grenoble INP, Institut NEEL, 38000 Grenoble, France
[4] Central European Institute of Technology, Brno University of Technology, 61200 Brno, Czech Republic
[5] Université Paris-Saclay, CNRS, Centre de Nanosciences et de Nanotechnologies, 91120 Palaiseau, France

[†] These authors contributed equally to the work
* Corresponding author: dedalo.sanz@cnrs-thales.fr

Keywords: Galton board, stochastic, domain-wall, nanomagnetic, neuromorphic, computing

Magnetic domain-walls travelling through a magnetic circuit[1] perform naturally and simultaneously logic and memory operations, eliminating the von Neumann information bottleneck[2]. The motion of magnetic domain-walls along nanoscale tracks is thus promising to achieve high-speed, low-power and non-volatile information processing, and an extensive range of domain-wall-based logic architectures is being explored[3–6]. Traditional domain-wall devices suppress intrinsic stochastic processes to enhance accuracy[7,8]. Still, domain-wall stochasticity could be turned into an asset by using stochastic computing frameworks, such as Bayesian sensing[9] or random neural networks[10]. These approaches however require controlling and tuning stochasticity. An iconic device used to illustrate the emergence of order from controlled randomness is the Galton board[11]. In this device, multiple balls fall into an array of pegs to generate a bell-shaped curve that can be modified

via the array spacing or the tilt of the board. Here, we demonstrate the controllability of domain-wall stochastic processes by recreating this experiment at the nanoscale. Balls are substituted by magnetic domain-walls, and bifurcating nanowires recreate the array of pegs. By probing domain-wall propagation through such a structure a large number of times, we demonstrate that stochastic domain-wall trajectories can be controlled and fine-tuned. This result sets the foundations for an integration of stochastic computing frameworks into domain-wall devices, opening new paths towards post-Von Neumann spintronics.

A foreseen stalling of Moore's Law[12] and the success of brain-inspired artificial-intelligence hardware[13–16] have triggered an intense search for spintronic devices that can perform complex computational tasks efficiently[17]. Magnetic vortex nano-oscillators[15], magnetic domain-wall synapses[18], and spin-ice networks[19] are part of this emerging family of alternative physics-based computing platforms[17]. In magnetic domain-wall devices, non-volatile information storage, transfer, and processing can occur simultaneously through the controlled movement of oppositely magnetized regions in a magnetic track[1], placing such devices under intense investigation[3–6].

Stochasticity in domain-wall motion is highly detrimental for traditional Boolean logic applications, and great efforts have been made to inhibit it in devices[7,8]. However, a powerful set of stochastic computing frameworks exists and is under intense investigation. These frameworks function by generating and transforming probability distributions, and can efficiently deal with data in which uncertainty is intrinsically present, or with difficult optimization tasks[20–22]. In this context, the once detrimental DW stochasticity becomes an exploitable asset, in the form of a natural source of randomness directly deployable within

more complex architectures. Here, we demonstrate that domain-wall stochasticity is controllable and tuneable by recreating one of the iconic experiments in statistics: the Galton board[11].

Our nanoscale magnetic equivalent of a Galton board is composed of an elliptical domain-wall nucleation pad and a bifurcating network of $Ni_{80}Fe_{20}$ magnetic nanowires (Figure 1a), 25 nm thick and 200 nm wide (see Methods). Upon application of an external magnetic field in the x-y plane (H_1), the elliptical pad reverses and injects a domain-wall into the network. The domain-wall then travels downwards, taking a random decision at each node it encounters. Magneto-Optical Kerr Effect (MOKE) microscopy (Figure 1b, see Methods) reveals the path taken by the domain-wall. Figure 1c illustrates, for the domain-wall path in Figure 1b, the magnetic orientation of each segment in the board. The '?' symbol indicates the nodes where the domain-wall took a random decision.

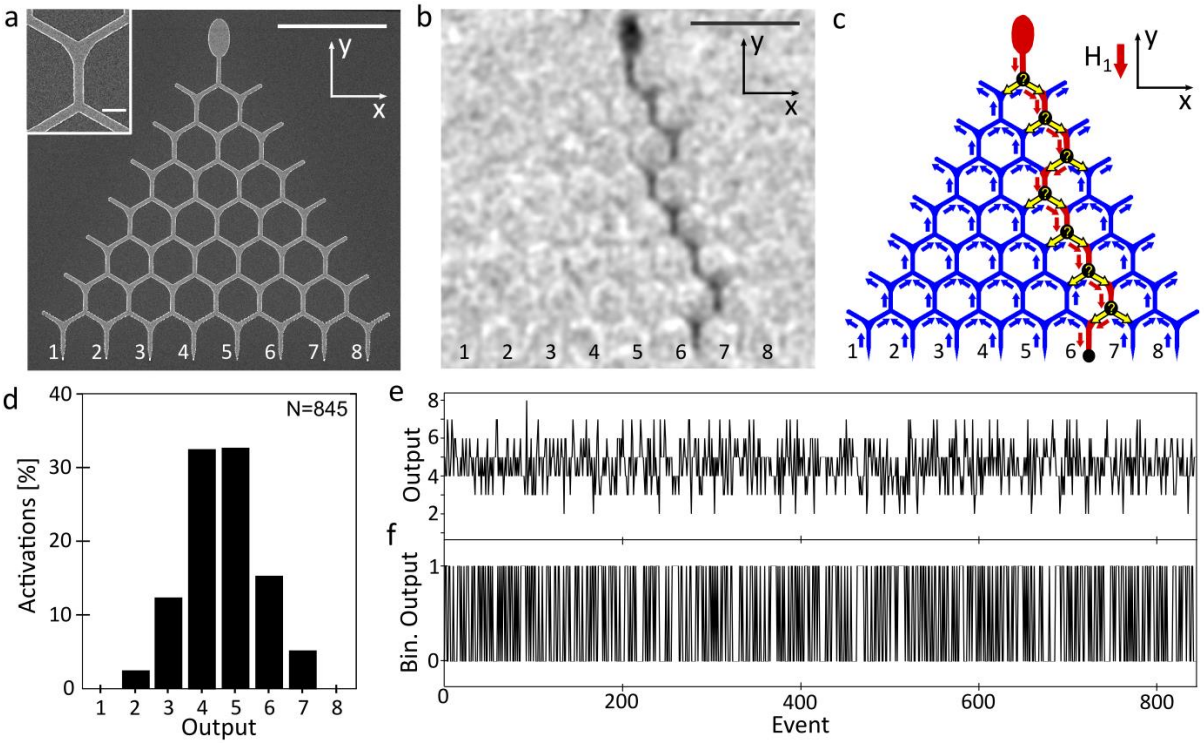

Figure 1: Nanoscale magnetic Galton board. (a) Scanning electron micrograph of a nanoscale magnetic Galton board composed by an elliptical nucleation pad at the top and a branching network of magnetic nanowires.

Inset: Round edges are employed at nanowire merging points to prevent domain-wall pinning. **(b)** Longitudinal Kerr Effect (MOKE) imaging of magnetic domain-wall propagation. **(c)** Schematics of the magnetisation reversal triggered by the domain-wall trajectory in (b). An 18mT uniaxial field (H_1) along the -y direction was employed to inject a domain-wall, which took a random decision at each node marked '?'. **(d)** Distribution of activated board outputs after N = 845 single-cascade events in 2,403 field cycles. **(e)** Order in which the 845 output activations occur. **(f)** Binarized output sequence employed to test randomness quality using the NIST test suite, obtained by mapping odd outputs in (e) to 0 and even outputs to 1. Scale bars: (a, b) 5µm, (a, inset) 500nm**.**

In this experiment, the detection of a large number of domain-wall propagation events is required. To achieve this, we optimize a full-field MOKE microscope (see Methods) to obtain 201,852 high-resolution magnetic images, a number hardly reachable by other means such as X-ray imaging or magnetic force microscopy. An automatic extraction of domain-wall paths from this large dataset allows us to precisely probe the properties of each node in the Galton board, the tuneability of the random process, and the degree of randomness in domain-wall path selection.

We first study domain-wall motion under symmetric conditions (Field H_1 along y), counting the number of times that a domain-wall reaches each of the eight outputs (Figure 1d). Stochastic domain-wall propagation is observed, with the distribution obtained approaching a binomial one. True stochasticity also requires independence between events in the time domain, i.e., the order of output activations (Figure 1e). For a quantitative evaluation of this degree of randomness, we binarized the sequence (mapping even outputs to 1, and odd outputs to 0, see Figure 1f) and passed it through the NIST Statistical Test Suite for Random and Pseudorandom Number Generators[23], which searches binary sequences for deviations from complete unpredictability. The sequence passes the 13 tests applicable to its length (see Methods), indicating that it comprises a highly uncorrelated set of random events. Another possibility in domain-wall systems is to have short-term memory, leading to correlations between subsequent domain-wall decisions[24]. Detailed trajectory analysis in the Galton board

reveals that no significant memory is present, which we associate to a chaotic interaction between magnetic vortices and anti-vortices in the domain-wall[25,26] (see Methods).

We continue by investigating the tuneability of the decision process at each node, a critical degree of freedom for the generation of arbitrary distributions. We define '*node probability*' as the probability of a right turn at a given bifurcation, and we evaluate how the node probability depends on the angle θ between the driving field H_1 and the y-axis (Figure 2a). Introducing this angle is the magnetic equivalent to misaligning a macroscopic Galton board with respect to the gravitational field.

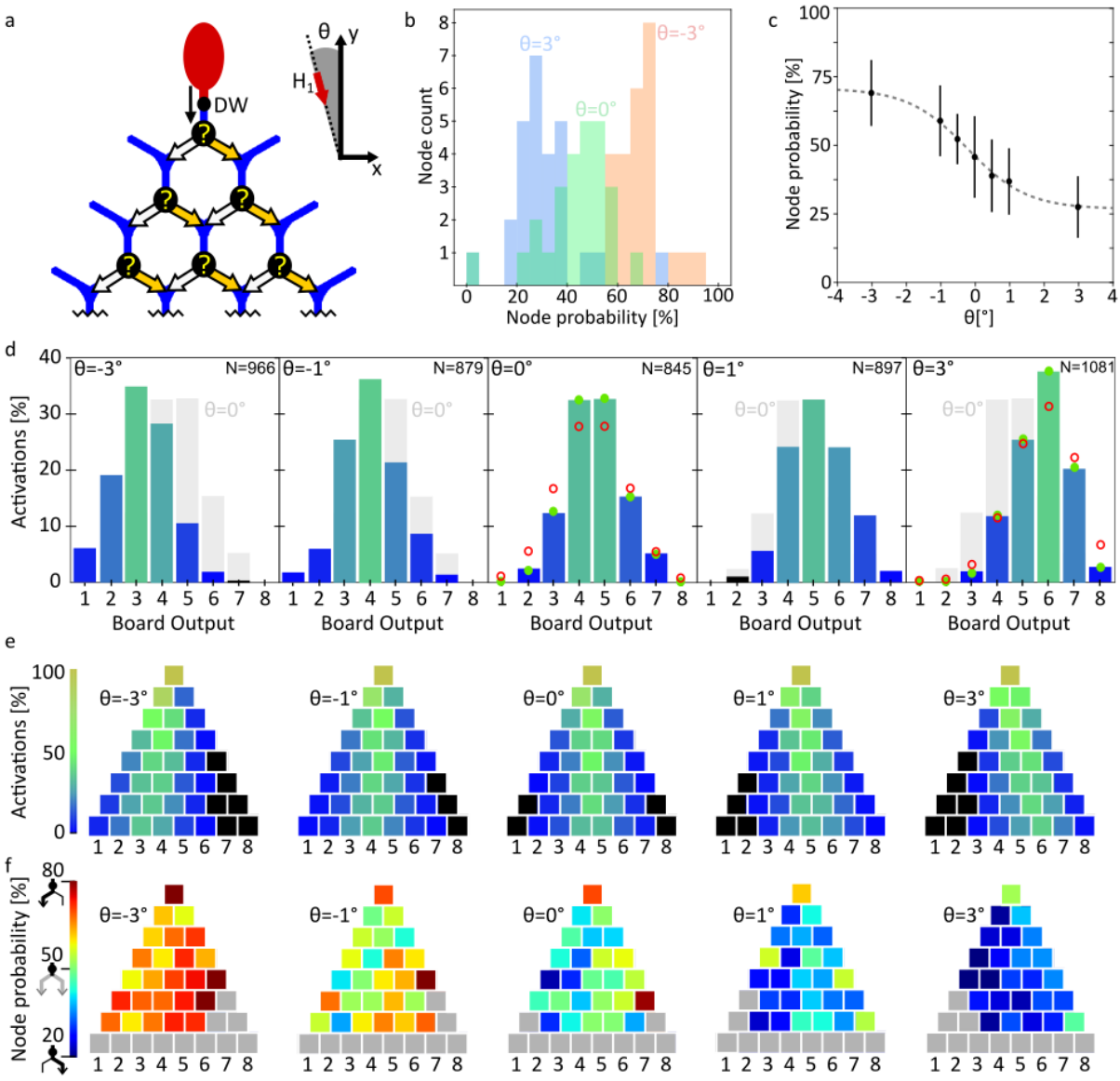

Figure 2: Tuneability of node probability. (a) The probability of a magnetic domain-wall (DW) for turning right at each node marked '?' (node probability) is controlled by tuning the angle between the applied field H_1 and the symmetry axis of the Galton board (y). A dark-yellow arrow indicates the direction (left turn) favoured by the angle θ in the diagram. **(b)** Histogram of node probability vs. field angle for the 28 nodes in the Galton board studied in Figure 1. **(c)** Mean and standard deviation of the distribution in node probability as a function of field angle θ. Dashed line: guide to the eye hyperbolic tangent fit. **(d)** Effect of field alignment on the magnetic Galton board output distribution. In colour: output distribution, light-grey shade: distribution at θ=0.0°. Colour follows the scale in (e). N indicates the number of events in each distribution after 2,403 field cycles. Red circles and green dots in panels θ=0.0° and θ=3.0° indicate the theoretically expected distribution for an ideal Galton board with the same probability in all nodes (red) and for a board in which each probability corresponds to the measured probability in panel (f) (green). **(e)** Spatial distribution of node activation as a function of θ. **(f)** Spatial distribution of node probability values. Confidence intervals given in Supplementary Figure 3. Grey nodes indicate impossibility to perform the measurement (insufficient counts/not-applicable). **(b-f)** ±0.3° experimental uncertainty in the alignment between the θ=0.0° direction and the y axis.

The structure studied contains 28 nodes, the first six marked '?' in Figure 2a, and as a MOKE image is available for each domain-wall propagation event, node probability can be studied for each node independently, at every field angle. We monitor first the overall evolution of node probability with θ. Figure 2b plots node probability for the 28 nodes as histograms, at θ = 0.0° (green), 3.0° (blue) and -3.0° (orange) respectively. We directly observe that a field tilt of 3.0° leads to a uniform bias in node probability of approximately 25 percentage units. Figure 2c displays the centre and standard deviation of the histograms for a larger number of field alignments, revealing that this bias is continuous and smooth in θ. Examining the output probability distributions (Figure 2d), a lateral shift of the distribution is observed as direct consequence of such uniform shift in node probability, analogously to the macroscopic case of a tilted board.

To confirm the behaviour, we further characterize the complete board (Figures 2e-f), looking at the number of trajectories that went through each node (Figure 2e) and evaluating locally all node probabilities (Figure 2f) by measuring the fraction of domain-walls that took a right turn. The expected tilting in the distribution of domain-wall trajectories is observed in Figure

2e, and a narrow distribution in node probability is observed at all fields (See also Figures 1b-c) with no obvious spatial correlations, indicating that variability between nodes is likely caused by small random differences during nanofabrication.

The red circles in Figure 2d show the expected output distribution of an ideal Galton board with uniform probabilities of 50% ($\theta = 0.0°$) and 68% ($\theta = 3.0°$) respectively. These red circles do not coincide with the observed distributions. However, if we calculate numerically the distribution resulting from cascading the individual node probabilities measured experimentally in Figure 2f, an accurate match is observed, represented by green dots in Figure 2d. This shows that the generated output distribution can be precisely computed by knowing the individual node probabilities, and can be controlled through these probabilities.

Results in Figure 2 set the foundations for creating devices in which node probability is tuned locally by means of electrical currents or geometrical modifications, to generate arbitrary output distributions. Given the wide and continuous tuneability range of node probabilities demonstrated (Figure 2e), generating an arbitrary probability distribution in such a device would only require a simple numerical optimization protocol.

Finally, we illustrate how the lattice structure can be engineered to further tune the output distribution and its normalization. In a complete board, all possible paths through the structure lead to an output, and therefore a consistent number of activations (N) is obtained at all operation angles. The structure in Figures 3a and b, however, breaks this condition by removing the central vertical element of the board and leaving the oblique elements marked *. These elements act as domain-wall sinks, preventing them from reaching an output and changing the resulting distribution. These sinks are the nanoscale equivalent to drilling a hole at the back of a macroscopic Galton board.

The measured consequences in the output distributions are presented in Figures 3c and d. At θ = 0.0°, a significant flattening of the distribution occurs compared to the complete board (see solid bars vs. grey lines), as well as a reduction of the number of detected events N. For tilted fields, the lateral shift of the output distribution is larger than in the complete board, while the reduction in N is less pronounced. These effects can be directly correlated to the number of domain-walls that travel through the central segment in Figure 2e, i.e., a reduction of 50% in N is observed at θ = 0.0°, whereas a reduction of 30% in N is observed at θ = ±3.0°. In future devices, strategic positioning of domain-wall sinks or stochastic pinning traps may be exploited in addition to node probability tuning to control the output distributions.

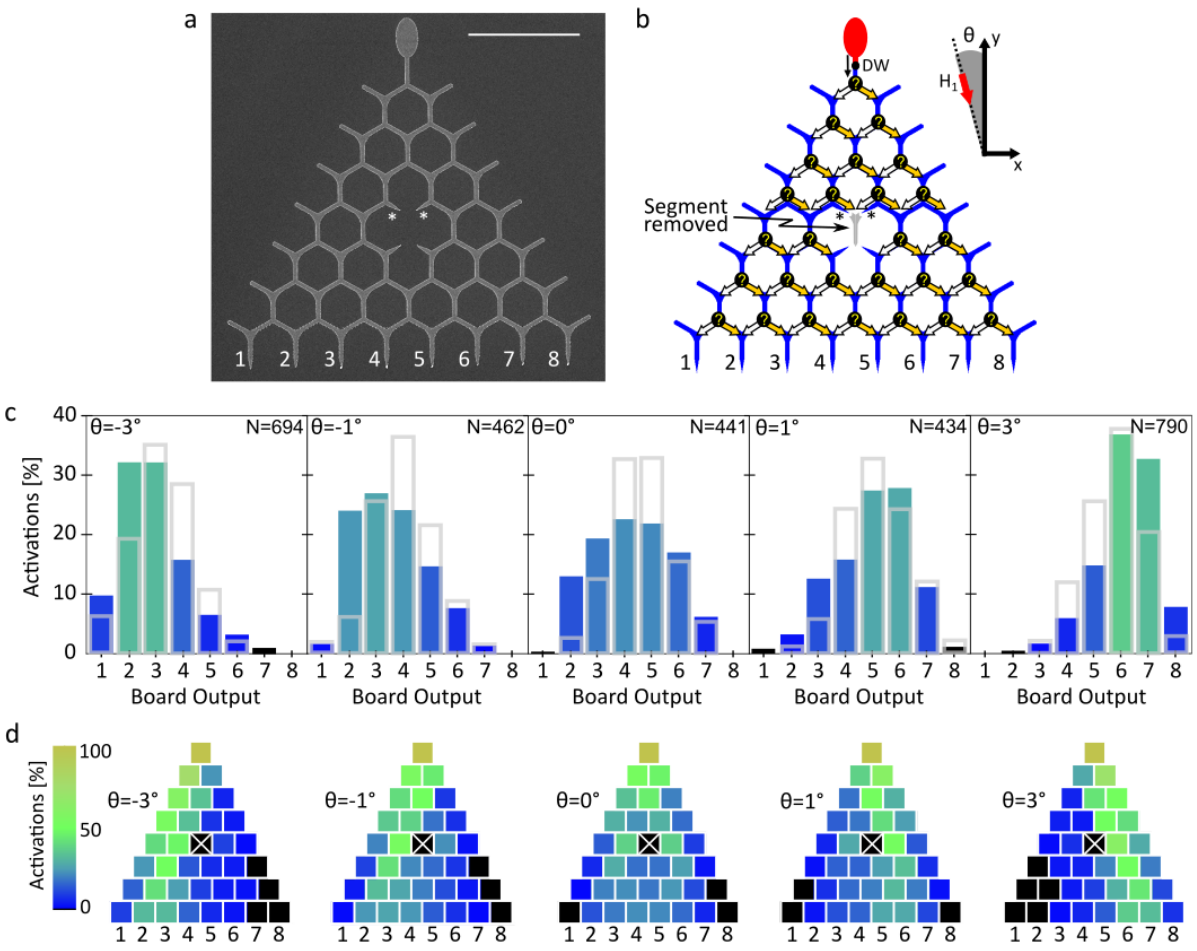

Figure 3: Galton board lattice edition. (a) Scanning electron micrograph of a nanomagnetic Galton board with a missing central element. The segments marked '*' act as domain-wall sinks. **(b)** The probability of a magnetic domain-wall (DW) for turning right at each node marked '?' (node probability) is controlled by tuning the angle

between the applied field H_1 and the symmetry axis of the Galton board (y). **(c)** Effect of field alignment θ on the distribution of output activations. Grey lines display the distribution of a complete board. N indicates the number of events in the distribution after 2,403 field cycles. **(d)** Spatial distribution of node activation as a function of θ. The node removed is indicated with a white cross. Scale bar: 5μm.

In conclusion, the suitability of magnetic domain-walls to generate and sample tuneable probability distributions is demonstrated by evaluating key randomness metrics in a nanoscale magnetic Galton board. Continuous tuneability of the domain-wall path-selection process is achieved and highly-uncorrelated randomness is demonstrated in the time and space domains. Further tuneability is achieved by using domain-wall sinks, which selectively destroy domain-walls passing through some nodes. These results extend the range of applicability of magnetic domain-walls beyond deterministic computing, opening their use as information carriers in high-speed non-volatile stochastic devices.

Acknowledgements. We acknowledge financial support from the ANR (ANR-17-CE24-0007), the Region Grand Est through its FRCR call (NanoTeraHertz and RaNGE projects), by the impact project LUE-N4S part of the French PIA project "Lorraine Université d'Excellence", reference ANR-15IDEX-04-LUE and by the "FEDER-FSE Lorraine et Massif Vosges 2014-2020", a European Union Program. D.S.H. and J.G. acknowledge support by DOE BES Award # DE-SC0019273 (Kerr microscopy, numerical data analysis and manuscript writing) for Q-MEEN-C, an Energy Frontier Research Center funded by the U.S. Department of Energy (DOE), Office of Science, Basic Energy Sciences (BES). We thank I. Soldatov and R. Schäffer (Evico Magnetics GmbH) for their support with Kerr microscope maintenance and software customization.

Author contributions. JG, FM, MM, MH and DL conceived the study. MM and FM fabricated the samples assisted by MH and DL. MM, FM, MH and DL optimized sample design using magnetic force microscopy experiments by MM and KB. FM and DSH performed exploratory micromagnetic simulations. V.S. and N.Ro performed exploratory MFM measurements. DSH

designed, optimized and performed the Kerr experiments assisted by NRe. DSH performed the data analysis. DSH wrote the manuscript with input from all authors.

Financial Interests. The authors declare no competing financial interests.

References

1. Hrkac, G., Dean, J. & Allwood, D. A. Nanowire spintronics for storage class memories and logic. *Philos. Trans. R. Soc. A Math. Phys. Eng. Sci.* **369**, 3214–3228 (2011).

2. Beyond von Neumann. *Nature Nanotechnology* vol. 15 507 (2020).

3. Allwood, D. A. *et al.* Magnetic domain-wall logic. *Science (80-.).* **309**, 1688–1692 (2005).

4. Parkin, S. & Yang, S.-H. Memory on the racetrack. *Nat. Nanotechnol.* **10**, 195–198 (2015).

5. Franken, J. H., Swagten, H. J. M. M. & Koopmans, B. Shift registers based on magnetic domain wall ratchets with perpendicular anisotropy. *Nat. Nanotechnol.* **7**, 499–503 (2012).

6. Luo, Z. *et al.* Current-driven magnetic domain-wall logic. *Nature* **579**, 214–218 (2020).

7. Muñoz, M. & Prieto, J. L. Suppression of the intrinsic stochastic pinning of domain walls in magnetic nanostripes. *Nat. Commun.* **2**, (2011).

8. Broomhall, T. J., Rushforth, A. W., Rosamond, M. C., Linfield, E. H. & Hayward, T. J. Suppression of Dynamically Induced Stochastic Magnetic Behavior Through Materials Engineering. *Phys. Rev. Appl.* **13**, (2020).

9. Ji, S., Xue, Y. & Carin, L. Bayesian compressive sensing. *IEEE Trans. Signal Process.* **56**, 2346–2356 (2008).

10. Timotheou, S. The random neural network: A survey. *Comput. J.* **53**, 251–267 (2010).

11. Chernov, N. & Dolgopyat, D. The Galton board: Limit theorems and recurrence. *J. Am. Math. Soc.* **22**, 821–858 (2008).

12. Leiserson, C. E. *et al.* There's plenty of room at the Top: What will drive computer performance after Moore's law? *Science (80-.).* **368**, eaam9744 (2020).

13. Merolla, P. A. *et al.* A million spiking-neuron integrated circuit with a scalable communication network and interface. *Science (80-.).* **345**, 668–673 (2014).

14. Prezioso, M. *et al.* Training and operation of an integrated neuromorphic network

based on metal-oxide memristors. *Nature* **521**, 61–64 (2015).

15. Torrejon, J. *et al.* Neuromorphic computing with nanoscale spintronic oscillators. *Nature* **547**, 428–431 (2017).

16. Ambrogio, S. *et al.* Equivalent-accuracy accelerated neural-network training using analogue memory. *Nature* **558**, 60–67 (2018).

17. Grollier, J. *et al.* Neuromorphic spintronics. *Nat. Electron.* (2020) doi:10.1038/s41928-019-0360-9.

18. Siddiqui, S. A. *et al.* Magnetic Domain Wall Based Synaptic and Activation Function Generator for Neuromorphic Accelerators. *Nano Lett.* **20**, 1033–1040 (2020).

19. Skjærvø, S. H., Marrows, C. H., Stamps, R. L. & Heyderman, L. J. Advances in artificial spin ice. *Nat. Rev. Phys.* **2**, 13–28 (2020).

20. Mizrahi, A. *et al.* Neural-like computing with populations of superparamagnetic basis functions. *Nat. Commun.* **9**, 1–11 (2018).

21. Alaghi, A., Qian, W. & Hayes, J. P. The Promise and Challenge of Stochastic Computing. *IEEE Trans. Comput. Des. Integr. Circuits Syst.* **37**, 1515–1531 (2018).

22. Camsari, K. Y. *et al.* From Charge to Spin and Spin to Charge: Stochastic Magnets for Probabilistic Switching. *Proc. IEEE* **108**, 1322–1337 (2020).

23. Rukhin, A., Soto, J. & Nechvatal, J. A Statistical Test Suite for Random and Pseudorandom Number Generators for Cryptographic Applications. *Nist Spec. Publ.* **22**, 1/1--G/1 (2010).

24. Pushp, A. *et al.* Domain wall trajectory determined by its fractional topological edge defects. *Nat. Phys.* **9**, 505–511 (2013).

25. Walton, S. K. *et al.* Limitations in artificial spin ice path selectivity: The challenges beyond topological control. *New J. Phys.* **17**, (2015).

26. Tretiakov, O. A., Clarke, D., Chern, G. W., Bazaliy, Y. B. & Tchernyshyov, O. Dynamics of domain walls in magnetic nanostrips. *Phys. Rev. Lett.* **100**, 127204 (2008).

27. Tanaka, G. *et al.* Recent advances in physical reservoir computing: A review. *Neural Networks* vol. 115 100–123 (2019).